Measurement of Water Absorption Cross-Sections for the Exploitation of GOME Data

EXECUTIVE SUMMARY
of
FINAL REPORT

August 2000

Study Team

Dr R.C.M. Learner (Scientific Lead)
Dr R. Schermaul
Mr G.S. Jones-Gilbey

Imperial College of Science,
Technology and Medicine
Blackett Laboratory
Prince Consort Road
London SW7 2BZ
UK

Dr J Ballard
Dr D Newnham
Dr K. M. Smith

Rutherford Appleton Laboratory
Chilton
Didcot
Oxfordshire
OX11 0QX
UK

Prof J Tennyson
Dr N.F. Zobov

Department of Physics & Astronomy,
University College London,
Gower Street
London WC1E 6BT
UK

ESA Officers:

Dr Jörg Callies, PT/APP

Mr Michael Eisinger, PT/APP

ESA/ESTEC
PO Box 229
2200 AG Noordwijk
The Netherlands

Study Manager

Mr M.G. Wickett

Serco Europe Limited
5th Floor, Kempton Point
68 Staines Road West
Sunbury-on-Thames
Middlesex TW16 7AX
UK

LIST OF CONTENTS

List of Figures

List of Tables

1 INTRODUCTION

Background

The GOME instruments, and their successor SCIAMACHY, are downward looking satellite borne spectrometers that observe the spectrum of the earth's atmosphere. Data covering a large number of species can be recovered from their observations. Although Ozone is the most important specie, other species are also of similar interest.

Water vapour is of particular significance. This is because it dominates the energy balance of the atmosphere. Also it is essential that the masking effects, due to the spectra of major constituents such as water vapour, be fully understood and accounted for when deriving the concentration or distribution of the minor components of the atmosphere.

Figure 1 is taken from a standard textbook on atmospheric science. This figure shows that within the visible from 395 to 765 nm, and the near infra-red from 765 to 1500 nm, only three molecules absorb significant energy: oxygen, ozone and water. The dominant member of this group, and the most variable, is water. It follows that any study of the atmosphere in the region around the Sun's maximum power emission must be able to adequately account for the effects of water vapour.

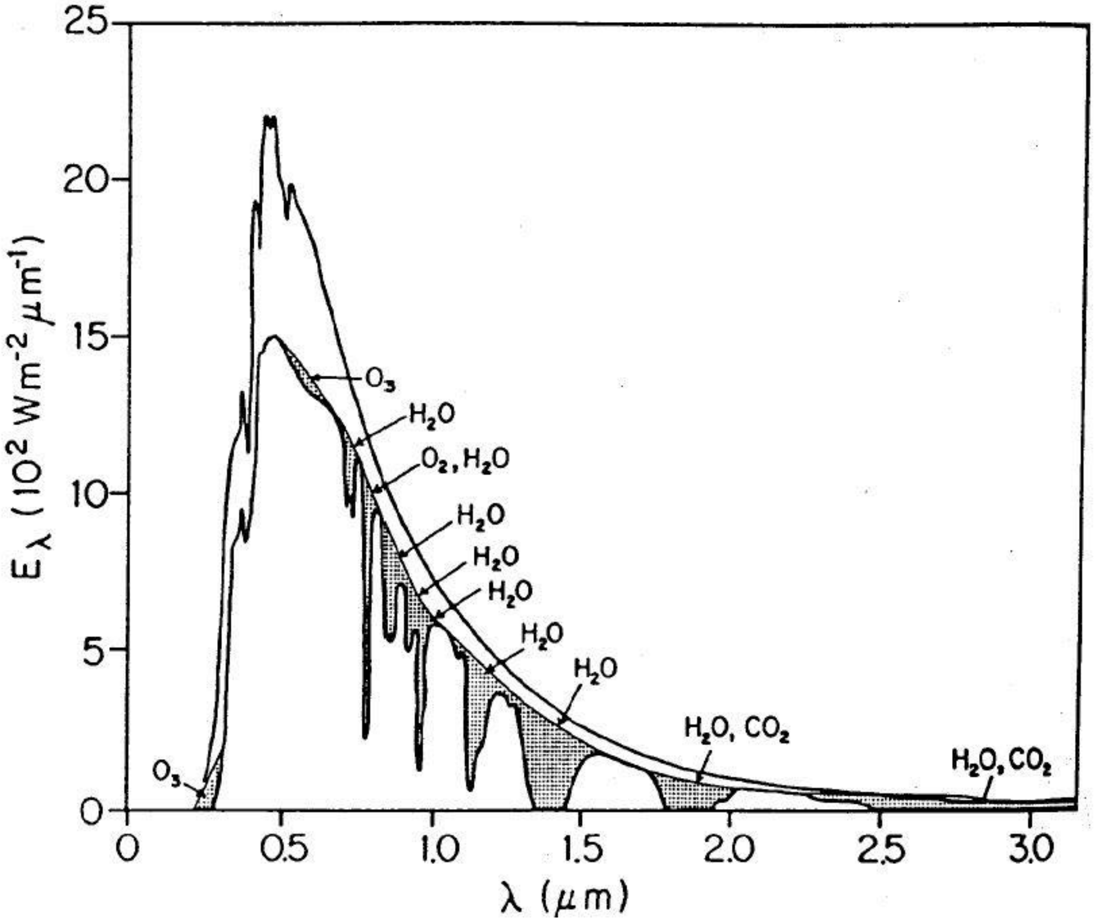

Figure 1: **Low resolution spectra of the sun**
(a) Above the atmosphere (upper line)
(b) At sea level, showing the principal absorption bands due to atmospheric gases (lower line)

(Taken from "The Physics of Climate", by Piexoto and Oort, American Inst of Physics, New York, 1992.)

Measurement: Objectives, Problems and Strategy

In the first instance, quantitative knowledge of the water spectrum must be derived from laboratory study. This is because only in the laboratory is it possible to observe the absorption spectrum at well-defined temperature and pressure. The principal practical problem for laboratory measurement is that the atmosphere contains a great deal more water vapour than can easily be studied in the laboratory. The atmospheric path is many kilometres, the limit of pathlength in the laboratory is a few hundred metres. Many weak lines that are too faint to be measured in the laboratory contribute significantly to atmospheric absorption: data on these lines must be generated using highly sophisticated theory.

It is believed that our study is the first in which experimental measurement of strong lines has been combined with theory-based computation for the weak lines. This technique enables a database for the water vapour spectrum to be provided, which is essentially complete in the context of GOME and SCIAMACHY retrievals.

Two fundamental problems affected the measurement and analysis strategy employed in this study: non-linearity and complexity.

Non-linearity occurs because, both for GOME and in the laboratory, the recorded parameter from observations of the water spectrum is the Intensity (the energy) detected at a specific wavelength whereas the required molecular property, which is a constant for each feature in the spectrum, is the Cross-Section. The Cross-Section is related to the logarithm of the Intensity: this is a very non-linear function.

This non-linearity is present at the most detailed level; the cross-section varies across the profile of a single absorption line. So even for a line, the relation between the overall energy absorbed and the measured molecular property is not simple. In practice it is quite common to find lines in the spectrum, where the cross-section at line centre is high enough to make the atmosphere completely opaque at that wavelength, while there are regions in the wings of these lines that are only partly absorbing. Under these circumstances it is essential that the line profile be known if the atmospheric transmission is to be accurately computed.

Complexity is illustrated in Figures 2 to 4. These show the water spectrum at different levels of detail. Figure 2 shows the spectrum for the near infrared and red region wavelength range 8500 cm^{-1} to 15500 cm^{-1} (1180 nm to 645 nm), at known temperature, pressure and path length. The spectrum shows a series of absorption bands, each of which is assigned to a superposition of several, quasi-degenerate, upper state vibrational levels, called a polyad. Figure 3 shows one band, due to the polyad of energy around 12000 cm^{-1}. Figure 4 shows a range of just 100 cm^{-1} (6.8 nm) near that band centre. Figures 5 and 6, from a spectrum taken at 252 K, show that the intensities and (less clearly) the line profiles are functions of temperature. If the energy levels are known, the variation of intensity can be computed; change in line profile must be determined experimentally.

The GOME and SCIAMACHY spectrometers cannot see the extremely fine detail shown in the figures above. Figure 7 shows the red end of a GOME spectrum. The smallest resolved spectral element, a GOME pixel, includes the effect of several of the experimentally observed lines, plus many more lines too weak for experimental observation. The new database, which is the primary product of this study, suggests that in the region covered by Figure 4, the average pixel records the sum of perhaps 100 water lines.

The combined effects of non-linearity and complexity are such that, to determine the absorption due to water at one pixel in the GOME spectrum, for the primary input to each atmospheric level in the model atmosphere used in the interpretation of the observation, it is necessary to evaluate non-linear summations over the profiles of each line, and then evaluate a second non-linear summation over all the lines included in that pixel,.

It is only possible to do this if every detail of the water spectrum observed in the laboratory is fully resolved. Convolution can always generate the effects of lower resolution. This is a one-way process: high-resolution data cannot be derived from a low-resolution observation. Without precise data on the molecule at this level of detail, the information derived from any atmospheric model will be seriously degraded. Differential studies, designed to bring out features concealed by the water absorption, will be almost impossible.

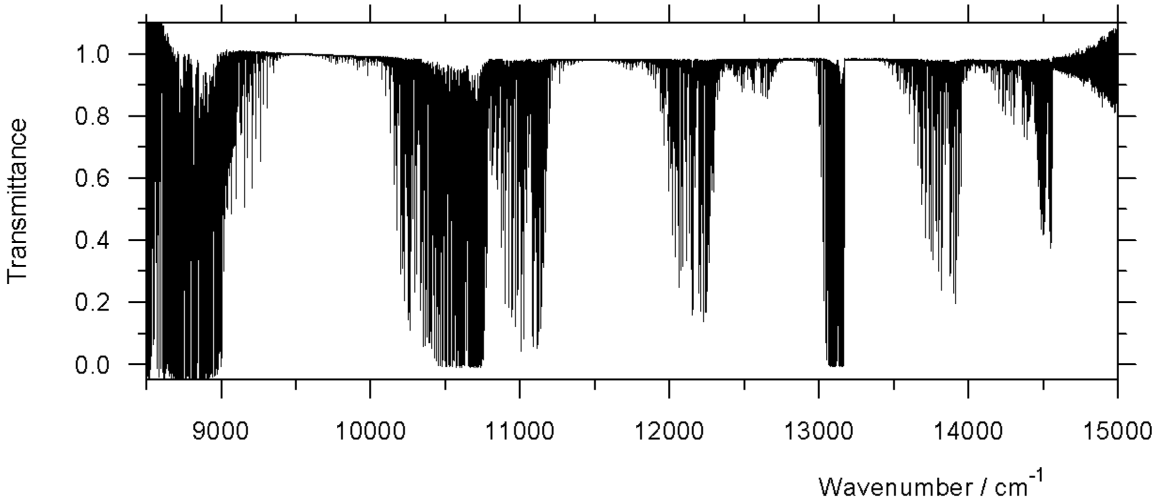

Figure 2 (a): **Plot of normalised transmitted energy versus wave number. The energy is shown in units normalised such that the absorption-free background has unit transmittance.**

Spectra are of a water vapour (10 hPa) / air mixture, with 1000 hPa total pressure, 293 K temperature, and an absorption path length of 512.75 metres.

Figure 2 (b) **Extension of the main observation shown in Figure 2 (a). This extension has an improved signal to noise ratio. (The band at 13200 cm^{-1} is due to oxygen, not water vapour.)**

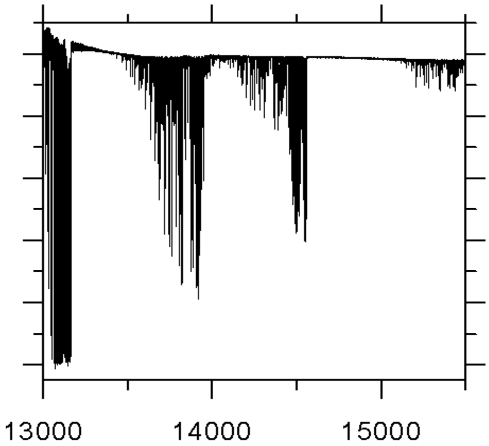

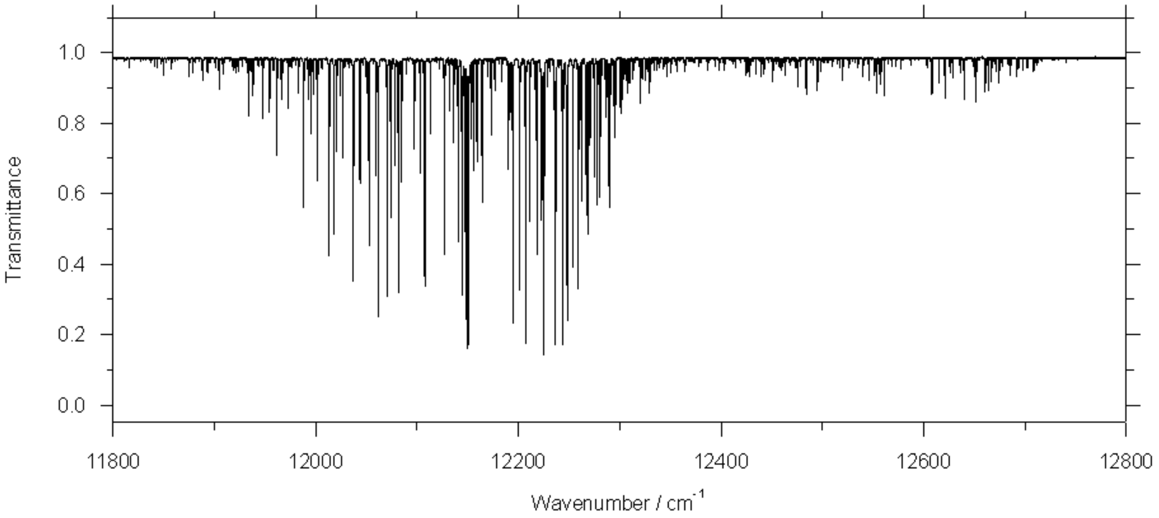

Figure 3: **A 1000 cm^{-1} section of the spectrum shown in Figure 2, showing a single polyad (3**n+ d)

Spectra are of a water vapour (10 hPa) / air mixture, with 1000 hPa total pressure, 293 K temperature, and an absorption path length of 512.75 metres.

Figure 4: **A 100 cm^{-1} section of spectrum shown in Figure 3, with individual line profiles just resolved**

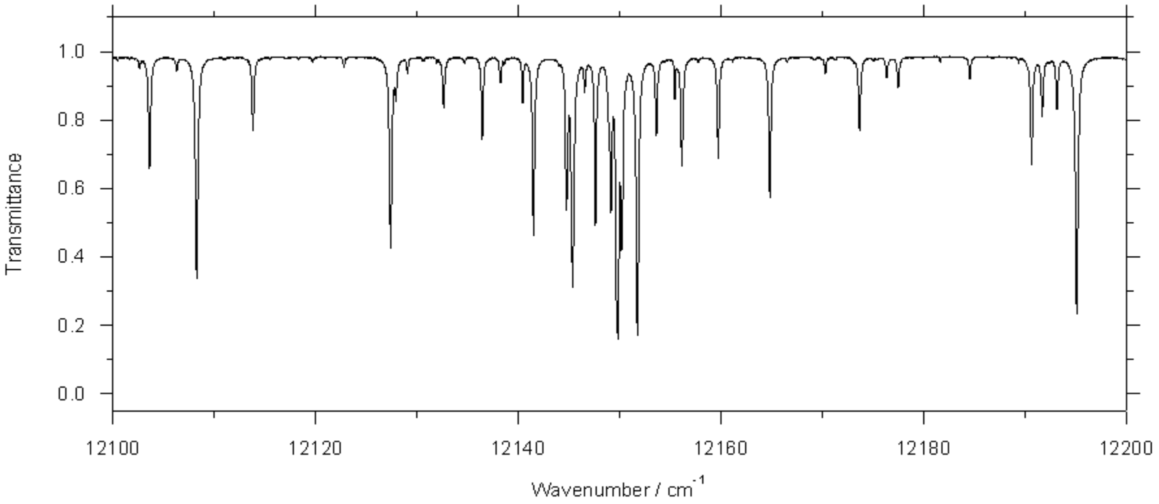

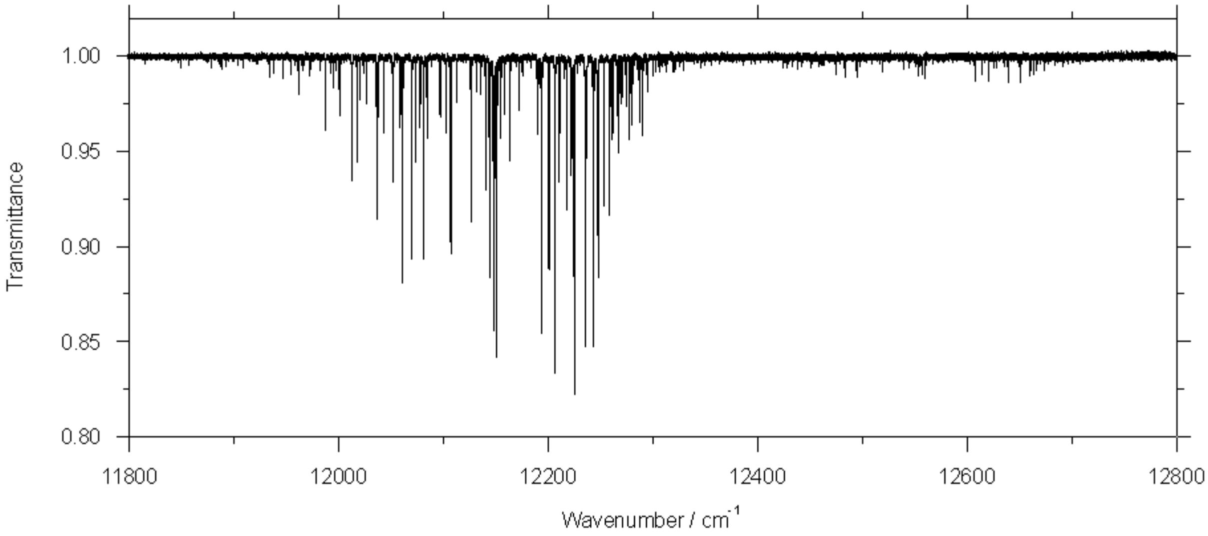

Figure 5: **Spectrum of the same polyad as in Figure 3, but at 253 K**

a) Spectra are of a water vapour (10 hPa) / air mixture, with 1000 hPa total pressure, 253 K temperature, and an absorption path length of 512.75 metres.

b) Note change of transmittance scale: the lines are very much weaker, due to the low partial pressure of water at this temperature.

Figure 6: **Same section of the spectrum as shown in Figure 4, but at 253 K**

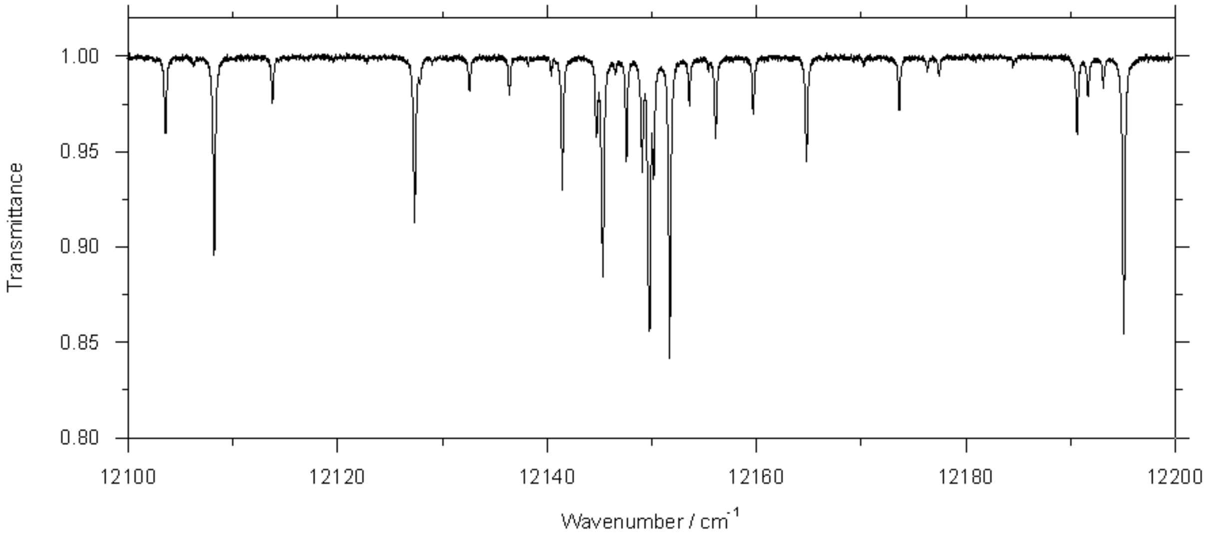

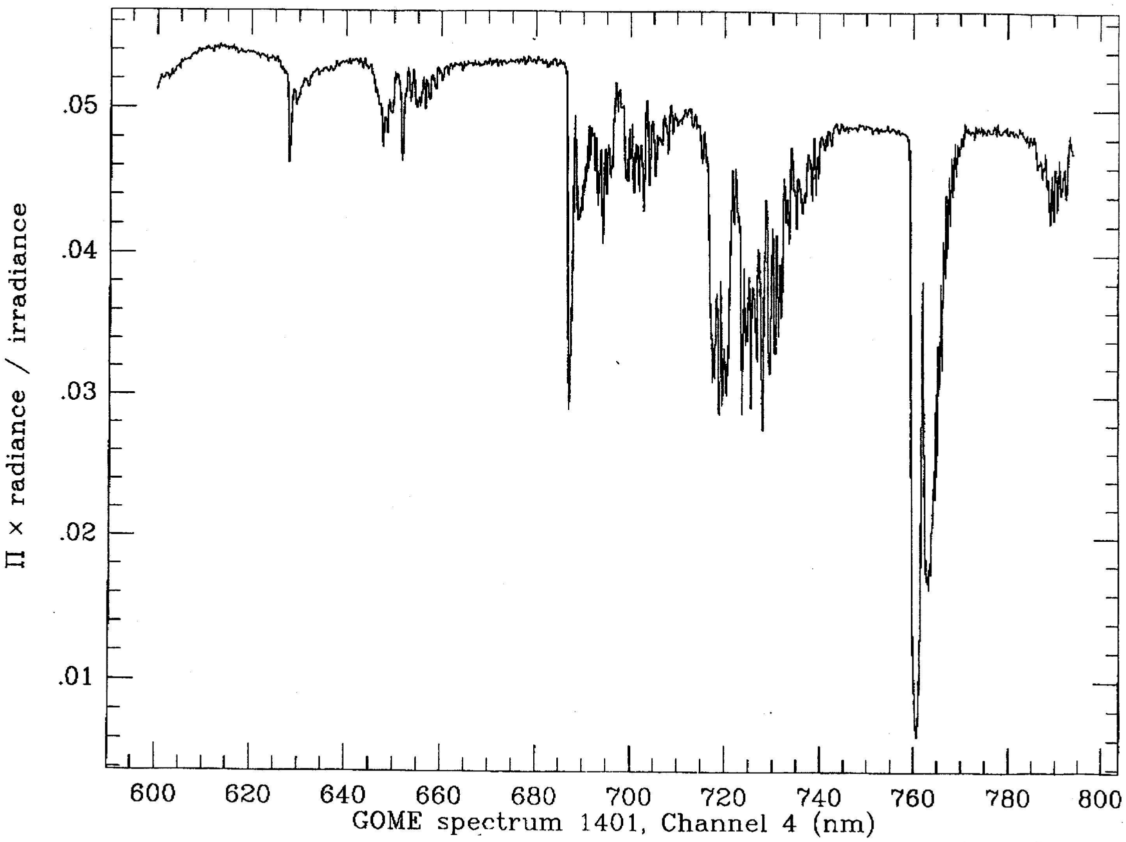

Figure 7: **Long wavelength end of a GOME spectrum.**

The strong double feature at 760nm, the spike at 687 nm and the weak spike at 627 nm are due to Oxygen. All other features are due to water.

Consideration of existing HITRAN database

An extensive database for the water molecule already exists. It is presented in its most accessible form as part of the larger atmospheric spectrometry database, HITRAN. The current edition, at the start of this contract was HITRAN96. The preliminary work undertaken during the preparation of a proposal for the upgrade of this database suggested that, while many features of the database, such as the wavenumbers of the lines and the assignments, were in excellent shape or had been upgraded since the publication of HITRAN96, some areas showed significant weakness.

The two most important concerns were the profiles of the strong lines and the positions and strengths of many thousands of lines below the detection limit of the experiments that underlay the database.

Our Consortium

In response to the ESA ITT for the present study, a consortium of three groups, which were already all working on the spectroscopy of water, agreed to combine with Serco providing project management. The three groups were:

- The Molecular Spectroscopy Facility at the Rutherford Appleton Laboratory (RAL), which has the necessary experimental facilities and expertise in measuring quantative, high-resolution spectra
- The Spectroscopy Group at Imperial College (IC), with expertise in the analysis of high-resolution molecular spectra
- The Molecular Theory Group at University College London (UCL), the leading group on the theory of the water molecule.

The result was a successful proposal for a two-pronged attack, which addressed the problems of profiles of strong lines, and the characteristics of the weak lines. Originally the measurement of the strengths of the strong lines was considered a relatively low profile task, though an essential stage in the data reduction. What was not anticipated was that this measurement would show that the HITRAN database had serious systematic errors, very much greater than the stated errors of the present study. As a consequence, there was a shift of emphasis. Much increased effort was invested in the evaluation of the errors of our own work, and in the preparation of a new database, rather than preparing an extension and improvement of the old one.

The remainder of this Executive Summary will follow the structure of the main Final Report: discussing first the review of the literature on the water vapour spectrum, then moving on to the experimental work, then addressing the theory, and finally ending with the combination of experimental and theoretical results into a single database and the comparison of this new data with the existing literature.

2 SURVEY OF LITERATURE ON THE WATER SPECTRUM

Measurement techniques

The literature review in this report comes at a critical point in the evolution of the relevant technology. There is no doubt that classical grating spectrometry is no longer of significance in the laboratory study of the water spectrum, and there are no data still in use that rely on the method. On the other hand, a group of laser-based techniques, using tuneable lasers are very sensitive and are of great promise. None of these new methods have yet progressed beyond the proof of principle level and none have yet been able to supply the wide wavelength coverage that is essential (a full list of references is given in the main report). The technology that dominates the field is high resolution Fourier Transform Spectrometry (FTS).

HITRAN Database

The HITRAN database is built on measurements made with Fourier Transform Spectrometry. Table 1 summarises the laboratory studies that underlie the HITRAN database. They are effectively a consistent set of studies, which are based on measurements made using the Fourier Transform Spectrometer and long path absorption cell at the US National Solar Observatory, in Tucson, Arizona.

Careful examination of this data shows that:

(i) All data are at room temperature and at absorption path lengths up to 434 metres,

(ii) Resolving power was sufficient to see the details of the line profile, and the wavenumbers are well determined

(iii) Signal to noise ratios are of order 500. So the weakest lines, of cross-section around 10^{-7} cm^2/atm, are not accurately characterised,

(iv) Many lines were not classified.

The main conclusions relevant to the work presented in this study are that there is no good data on weak lines, and that the data reduction methods used on the spectra in Table 1 did not generate good line profile data. Since the work was published in the mid to late 1980s, the majority of the unassigned lines have been classified.

During our study, a paper was published identifying several sources of systematic error in HITRAN96, which were due to defects in the conversion of the original laboratory data to the standard format used in HITRAN. However, this paper did not reconcile the discrepancies between our work and HITRAN. Although some data now fitted better, in many cases the disagreement was increased. The current state of the water vapour spectrum is best seen in the Proceedings of the June 2000 meeting to discuss the HITRAN database. In this meeting a whole session was devoted to the problems of the database for water.

Table 1: Summary of Published Data on the Water Vapour Spectrum

Polyad[(1)]	**Wavelength Range nm**	**Wave number Range cm^{-1}**	**Number of lines observed**	**Max Intensity cm^{-1}/(cm atm)**	**Min intensity cm^{-1}/(cm atm)**	**Ref**
3ν	1050-870	9500-11500	2413 [(2)]	1.5xE –2	2xE-7	(1)
3ν+δ	860-785	11600-12750	1239 [(2)]	1.1xE-3	7xE-7	(2) (3)
4ν	760-680	13200-14700	2185	3.2xE-4	2xE-7	(4)
4ν+δ	670-625	14900-16000	693	6.2xE-5	4xE-7	"
5ν	605-565	16550-17660	1027	6.7xE-5	4xE-7	(5)
5ν+δ	555-520	18060-19100	356	7.1xE-6	3xE-7	"
6ν & 6ν+δ	515-470	19500-21350	359	1.4xE-5	2xE-7	"
7ν & up	470-400	21350-25100	284	6xE-6	2xE-7	"
Overall	**1050-400**	**9500-25100**	**8556**	**1.5xE-2**	**2xE-7**	**-**

Notes:

(1) A polyad is a set of superposed bands for which n = v1 + v2/2 + v3, where v1, v2 and v3 are the vibrational quantum numbers of the excited state. If v2 is odd, n is the integer part of the sum, and a delta is added.

(2) Assigned lines only - at a rough estimate there are about 1400 additional lines that have been observed but were neither assigned nor published. Many of these lines have been assigned since the original publications summarised here.

(3) The full references are set out in Section 2.7 of the main Final Report

Pressure Broadening

A second section of the literature review concentrates on the relation between pressure broadening of the spectrum lines and the pressure of the foreign gas (usually air) that causes the broadening. Many examples were found to confirm that the relationship between line broadening and pressure is linear. This has immediate impact on the experimental strategy, as it supports a strategy in which careful measurement is made at high pressure, rather than using the observation time to make several lower quality measurements over a range of pressures.

3 EXPERIMENTAL WORK AND DATA ANALYSIS

Experimental Measurements

For reasons set out in the Introduction to this Executive Summary, the primary experimental requirements for the laboratory study of the water spectrum are a long path absorption cell and a high resolution Fourier transform spectrometer. These were provided by the Molecular Spectroscopy Facility at RAL.

The long path cells, which are available at RAL, are both White-type multi reflection cells in which high reflectance mirrors are used to fold paths of up to 512 metres into compact absorption systems. Both these cells have the considerable advantage that they can be cooled to temperatures comparable to those found in the upper troposphere (and if need be, down to 90 K). The cells can be connected to the very high-resolution Bruker spectrometer by using evacuated paths. The Bruker IFS 120HR is an instrument fully capable of resolving the extremely high detail in the water spectrum. In practice during this study, signal to noise ratios of up to 900:1 at resolution of 0.03 cm^{-1} were achieved.

With this signal quality, data with random errors of 1% or better can be retrieved for lines for which the transmittance lies between 0.17 and 0.72. Outside these limits, weaker lines have too low signal to noise ratio and stronger lines are beginning to saturate. It is necessary, therefore, to work at several different path lengths to cover the required dynamic range.

In total, sixteen high-resolution spectra were observed and analysed. These spectra were measured with path lengths of 5, 32, 128 and 512 metres. Measurements were made with both pure water vapour, and with a mixture of water vapour and approximately 1000 hPa of synthetic air (a CO_2 free, dry, O_2/N_2 mix). Observations were made at 293 K for all path lengths, and at 253 K for the longer paths. The water vapour pressure at 253 K is too low to give adequate absorption at the shorter paths.

A great deal of effort was put into the determination of the key parameters: water vapour pressure, path length and temperature. Of these the water vapour pressure measurements proved the most difficult. After careful comparison, humidity sensor readings were preferred over absolute manometry for deriving water vapour pressure.

The data generated in these observations are summarised in Table 2 below. Copies of the data were sent to IC for detailed analysis. These data have been archived at ESA, and are available to users who may wish to test our results or to derive other information.

Data Analysis

The first phase of the data analysis was to establish the zero and 100 % transmission levels for each spectrum.

Effects such as lamp aging combine with the long time needed to fill and empty the absorption cell to prevent this being done by taking the ratio of full to empty cell transmission. In practice a 100 % transmission level has to be established by fitting a smooth curve through the points where the water absorption is negligible. This is difficult, and can be the source of serious systematic errors. For this reason independent evaluations of the unabsorbed background intensity were made at RAL and IC and the results compared. The spectra were then transformed into absorbance, rather than intensity, units for further analysis.

The second stage of the analysis required the fitting of a four-parameter general (Voigt) line profile to each line in the spectrum. This is a slow process, even with a fast computer. This is because the fitting process is interactive, and relies on an operator to identify features that distort the fit: for example a weak line in the wing of a strong line, which the computer has assumed to be a single line. In the air-broadened spectra, where line blending is more prevalent and the line fitting particularly tedious, over 11 000 individual line profiles were fitted. Figure 8 shows a small section of one spectrum and plots the residuals from the fitting process.

Table 2: Experimental conditions of the water vapour measurements

Spectrum	**Sample**	**l (m)**	**T (K)**	**pH_2O (hPa)**	**ptot (hPa) a**
EWKC1T	H_2O	4.938 (13)	294.9 (5)	9.459 (44)a	9.459 (44)
EWKC3T	H_2O / Air	4.938 (13)	295.3 (5)	8.83 (28) b	999.29 (97)
EWGB1T	H_2O	32.75 (6)	294.4 (7)	10.017 (15) a	10.017 (15)
EWGB2T	H_2O / Air	32.75 (6)	296.2 (7)	9.10 (23) c	1003.6 (16)
EWIA8T	H_2O / Air	32.75 (6)	296.0 (7)	9.25 (14) c	1000.0 (12)
EWGC1T	H_2O	128.75 (18)	295.7 (7)	10.008 (11) a	10.008 (11)
EWGC2T	H_2O / Air	128.75 (18)	296.4 (7)	9.07 (23) c	999.9 (14)
EWIA7T	H_2O / Air	128.75 (18)	296.1 (7)	9.18 (15) c	1000.0 (11)
EWGD1T	H_2O	512.75 (66)	295.6 (7)	10.094 (11) a	10.094 (11)
EWGD2T	H_2O / Air	512.75 (66)	296.4 (7)	9.08 (21) c	1001.3 (10)
EWIA5T	H_2O	512.75 (66)	295.8 (7)	10.003 (11) a	10.003 (11)
EWIA6T	H_2O / Air	512.75 (66)	296.4 (7)	8.96 (42) c	1000.5 (13)
EWGF2T	H_2O	128.75 (18)	252.0 (7)	0.809 (2) a	0.809 (2)
EWGH1T	H_2O / Air	128.75 (18)	252.1 (7)	0.717 (10) c	998.7 (10)
EWGF1T	H_2O	512.75 (66)	251.0 (7)	0.816 (6) a	0.816 (6)
EWGG21T	H_2O / Air	512.75 (66)	251.1 (7)	0.713 (11) c	998.9 (11)

Notes:

(1) The numbers in parentheses are the error estimates in units of the last digit quoted

(2) a Pressure measurements using the MKS Baratron gauges.
b Pressure determined from the spectral analysis.
c Pressure measurements using the humidity sensors.

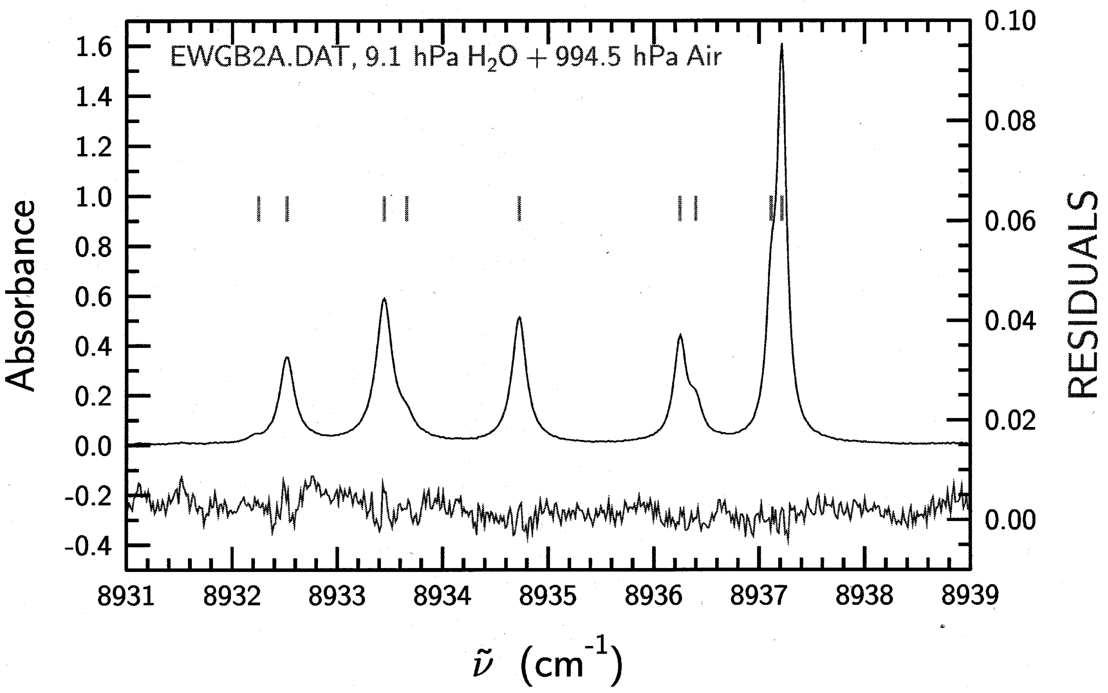

Figure 8: **Results of a spectral line-fit.**

The small vertical markers indicate the fitted lines in the spectrum (upper trace). The lower trace shows the residuals on an expanded scale.

The known temperature pressure and path length were combined with the list of fitted lines to generate cross-sections. Duplicated observation of the same line at different path lengths were then merged to give error-weighted best values of line strength and profile parameters for each line. This list was then given a thorough error analysis: about one third of the line strengths and broadening parameters are believed accurate to better than 2.5 %, well over half have errors less than 5 %. The final set of experimentally determined line parameters, covering some 5000 lines, is summarised in Table 3.

Further analysis of the lines in this list was then done to examine the variation of line broadening parameters with the rotational and vibrational quantum numbers. This was needed to give guidance on the expected widths of the weak lines that were the main product of the theoretical work.

Table 3: **Polyads, Wavenumber Ranges and numbers of Strong Lines**

Polyads	Wavenumber ranges cm^{-1}	Numbers of measured Strong Lines
$2\nu+\delta$	8592 - 9488	706
3ν	9651 - 11414	2447
$3\nu+\delta$	11589 - 12752	899
4ν	13403 - 14537	982

4 THEORETICAL WORK

Background

Over the last few years there have been major improvements in the theory of the water molecule spectrum. To a large extent these improvements have resulted from the fundamental strategy of changing from perturbation to variational methods. This change has been led by the group at UCL.

The theory is divided into two sections:

- Ab initio calculation of the molecular motion, which establishes the energy levels,
- Construction of the “dipole surface”, which allows the computation of intensities.

Observed and calculated energy levels now agree to a few parts in 10,000. This precision has been used firstly to classify the unassigned lines in earlier work, and secondly to very carefully check the assignment of all the lines observed in the experimental part of this study. Where necessary errors were corrected. In particular this affected a number of lines that had been assigned to H_2O^{18}, but proved to be weak transitions in H_2O^{16}.

Comparison of Measured Spectra and Spectra synthesised from derived line parameters

At this point a test was run to see how well the derived data could reproduce the original spectra experimentally measured at RAL. Figure 9 shows a section of the observed spectrum with the synthesised spectrum plotted beneath. Even with an expanded scale the differences are seen to be slight. Over the entire range above 9000 cm^{-1}, agreement is found to better than +/- 2%.

Figure 9: **Comparison of Observed Spectrum and Synthesised Spectrum**

Observed Spectrum ———
Synthesised Spectrum ....

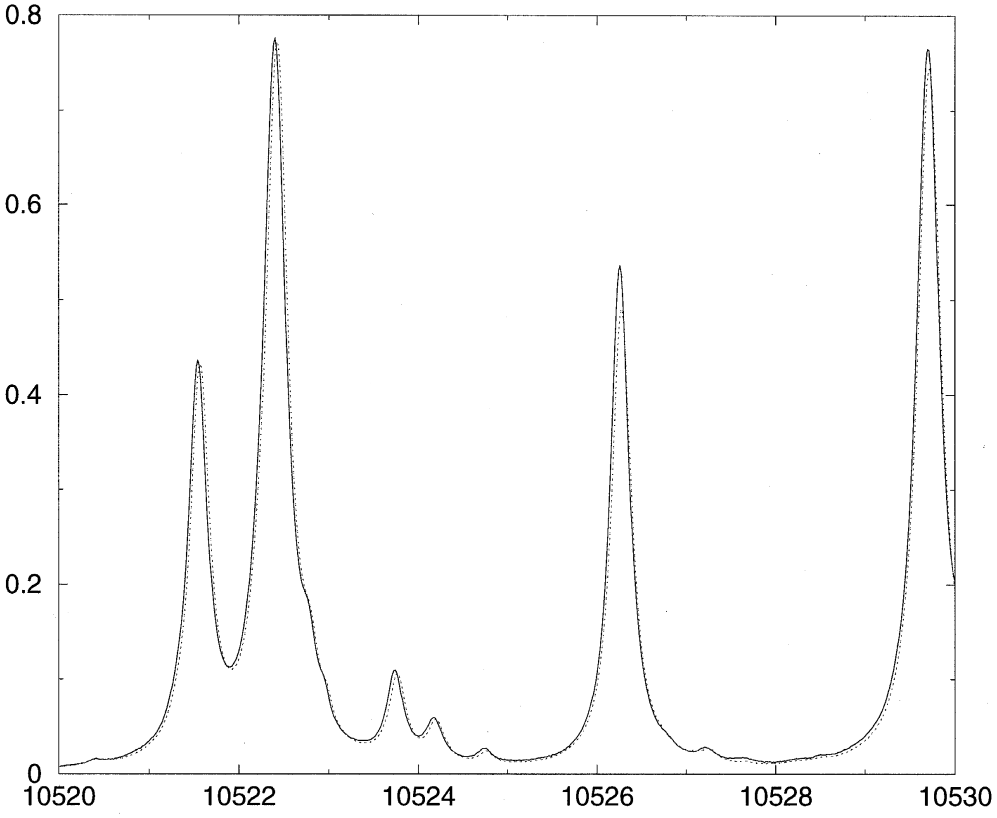

Computation of theoretical line strengths for ESA-WVR linelist (8592 cm^{-1} to 15000 cm^{-1})

Following the successful comparison for the strong lines, of measured and computed line strengths; the positions and strengths of all lines down to a certain minimum intensity were computed. This minimum intensity was chosen as a level where the total effect of all remaining weaker lines was negligible. The resulting list of computed strong and weak lines contained some 36000 lines.

The next step required input from the experimental work: the computed lines had finite strengths, but zero widths. The experimental data showed that width did not vary significantly with vibrational quantum number, but, on average, decreased steadily as the rotational quantum number increased. Figure 10 shows this variation for eight vibrational states in the 3ν polyad. Fortunately the precise detail of the profiles of the weak lines is not important: these lines are so weak that the linear relation x = log(1 + x) suffices.

Figure 10: Rotational dependence of the air-broadening coefficients for the 3n polyad.

(a) Average air-broadening for given lower state rotational quantum number (*J''*) value and vibrational transition, plotted against *J''*.

(b) Parameters for different vibrational transitions are displayed as different lines. The key label indicates the upper vibrational state ($v_1v_2v_3$); all transitions are from the ground state (000):

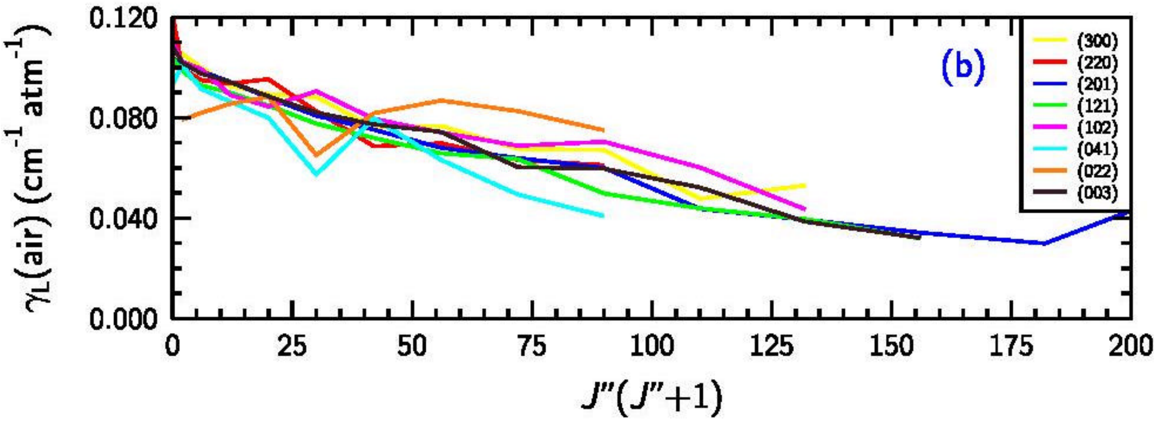

Computation of theoretical line strengths for ESA-WVB linelist (15,000 cm^{-1} to 20,000 cm^{-1})

In the region15,000 cm^{-1} to 20,000 cm^{-1} the lines are much weaker, which makes their accurate measurement in the laboratory much more difficult. However these weaker lines are easily observed as absorption in the atmosphere. For this reason, an additional theoretical list was generated to cover this region. This is known as the ESA-WVB linelist (B for blue).

This ESA-WVB linelist corresponds to transitions to polyads of high excitation. It should be noted that it lacks the same experimental validation as the ESA-WVR linelist. For this reason the ESA-WVB linelist should be treated with caution until further verification has been carried out.

5 FINAL LINE LIST AND COMPARISON WITH HITRAN.

Final ESA-WVR linelist (8592 cm^{-1} to 15000 cm^{-1})

The final ESA-WVR linelist was prepared by merging the corresponding experimental and theoretical inputs. The experimental data contributed about 4000 stronger lines, and the theory contributed about 32000 weaker lines. The list was compiled using the HITRAN format, so that it would be in a form familiar to the user community and easily assimilated into their models.

Each record in the linelist corresponds to a line and comprises the following parameters: line frequency, classification, energy levels, line strength and line broadening parameters for air broadening. HITRAN parameters, which were not measured within this study, are included in our new linelist: these include self-broadening effects and pressure shifts.

Table 4 indicates the numbers of measured (strong) lines and theoretical lines included in the new ESA-WVR list, and their distribution by polyad.

Table 4: Final Linelist: Total lines, "strong lines" and new assignments (by Polyad)

Polyad	Number of Strong Lines	Number of New Assignments	Number of $H_2{}^{18}O$ lines	Total Number of Lines
$2\nu+\delta$	633	30	0	6040
gap	(No "strong lines")			439
3ν	1897	281	23	12430
gap	(No "strong lines")			397
$3\nu+\delta$	715	134	0	6380
gap	(No "strong lines")			1659
4ν	910	142	0	7958
gap	(No "strong lines")			1297
Totals	4155	587	23	36600

Comparison of ESA-WVR linelist with HITRAN database

Comparison of the ESA-WVR linelist with HITRAN is essentially a comparison of the US National Solar Observatory based data of the 1980s and our new experimental measurements. This comparison shows large and unexpected discrepancies. Figure 11 gives an overview of the situation, and shows that the discrepancies, for the strongest lines, are dominated by systematic shifts that vary from polyad to polyad, while at the lower end of the intensity range, the random errors (principally in the older data, though our results below 8500 cm^{-1} are at poor signal to noise ratio) are often more than a factor of two. The inclusion of the recent corrections to HITRAN96 does not alter the pattern: some discrepancies increase, some decrease, but there is little net improvement.

.

Table 5: Comparison of integrated line intensities with HITRAN96.

Temperature	2n+ d	3n	3n+ d	4n
T=296K	1.26(2)	1.21(2)	1.25(2)	1.06(2)
T=252K	1.20(2)	1.27(2)	1.33(3)	1.12(3)

Notes:

a) The values given are ratios between the sum of the observed intensities and the sum of the corresponding HITRAN values

b) Blended lines, or missing lines in either linelist have been omitted.

c) Numbers in parentheses are the error estimates in units of the last digit quoted.

The error of the sum of the observed intensities is to first order determined by the errors of the strong lines, which are below 2.5%. This translates through standard error analysis to the errors given in this table. Due to a lack of knowledge, no error was assumed for the HITRAN data.

The results of this comparison had a considerable impact on the contract. We had set out with a view that the quoted errors of the line strengths in the HITRAN data were, in general, of the accuracy claimed: 5 % for the stronger lines. Systematic differences of some 30 % led to a very thorough re-examination of our own error budget, especially the difficulty of determination of the absolute water concentration. No errors were found that could explain the disagreement.

The inevitable conclusion was that a new database was a necessary consequence of the new data. The original plan had been to address two weaknesses of the HITRAN database, so that it could be improved and extended. It became clear that the most important component of the HITRAN list, the line strengths, were suspect and had to be replaced.

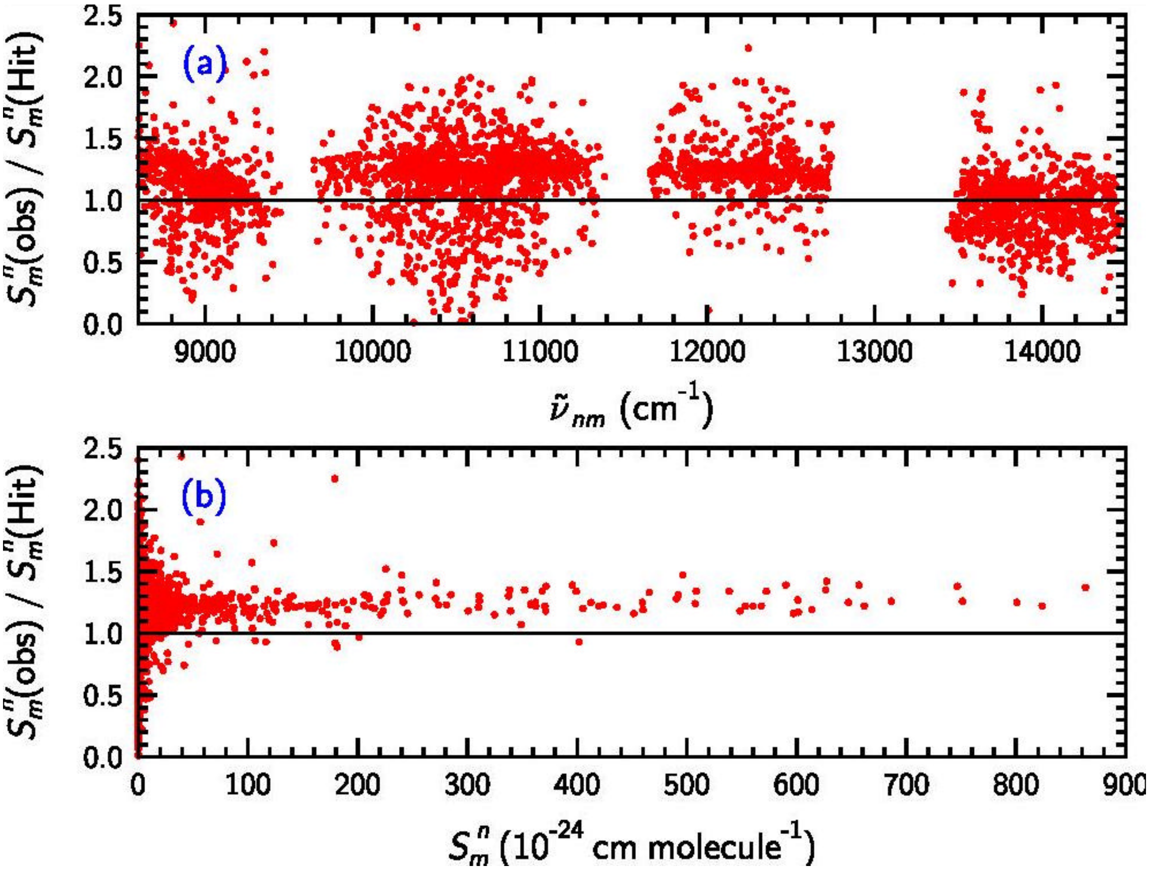

Figure 11: Comparison of integrated observed line intensities with HITRAN96 data

(a) Polyad-by polyad as a function of wavenumber (at room temperature)
(b) As a function of the line intensity (at room temperature)

6 CONCLUSIONS

Two new line lists have been constructed:

- ESA-WVR: covering the Near-IR and Visible region (8592 cm^{-1} to 15000 cm^{-1}). This line list was derived from a synthesis of state of the art theoretically derived data and experimental measurements carried out specifically as part of the present study.
- ESA-WVB: covering the Blue region (15000 cm^{-1} to 20000 cm^{-1}). This line list was derived from experimental measurements carried out by various workers (independent to the present study), with theoretical data added.

Both are included on the CD ROM that forms one of the contract deliverables. The great majority of the absorption due to water in the visible and near infrared is included in the principal list, ESA-WVR. The second list, ESA-WVB, provides data for the weak transitions in the short wavelength part of the visible region.

The ESA-WVR has been subjected to a very thorough error analysis. We believe that the data presented are a major improvement over the data in the current literature. It is significant that the new data differ from the old in the direction that much reduces the “missing opacity” of the atmosphere. This effect, which is a serious difference between the observed energy absorption by the atmosphere and the best theoretical models, has been the motivation for a very large research effort to identify unknown contributors to the atmospheric opacity. Weak lines, a major new component of our database, were known to be one contributor: the arguments for this were statistical. ESA-WVR gives wavenumbers, strengths and widths for the tens of thousands of lines involved, and so this contribution can now be modelled with confidence. The increase in measured line strengths for the strong lines was unexpected, but will also reduce the fraction of the opacity that is “missing”.

The primary purpose of the work was to improve the understanding of the water spectrum in order to enable a corresponding improvement in the interpretation of GOME data. This we feel we have achieved. The improvements are very much more important than we had envisaged at the start of the programme.

Our data are now available in a format that is familiar and well understood. The databases ESA-WVR and ESA-WVB, together with this Executive Summary can be downloaded from the following website:

NERC/BADC: http://www.badc.rl.ac.uk/data/esa-wv/

Additional information can be obtained from Dr Jörg Callies
(email: jcallie@estec.esa.nl).

Finally, we hope users will find our work both significant and useful.

7 PUBLICATIONS RELATING TO THE STUDY

At the time of writing this Final Report, the following papers/talks were in preparation, or had been submitted:

1. R. Schermaul, R.C.M. Learner, D.A. Newnham, J. Ballard, N.F. Zobov, D. Belmiloud and J. Tennyson, The water vapour spectrum in the region 8600-15000 cm^{-1}: experimental and theoretical studies for a new spectral line database I: Laboratory measurements, *J. Molec. Spectrosc*, (to be submitted).
2. R. Schermaul, R.C.M. Learner, D.A. Newnham, J. Ballard, N.F. Zobov, D. Belmiloud and J. Tennyson, The water vapour spectrum in the region 8600-15000 cm^{-1}: experimental and theoretical studies for a new spectral line database II: Construction and validation, *J. Molec. Spectrosc*, (to be submitted).
3. D. Belmiloud, R. Schermaul, K. M. Smith, Nikolai F. Zobov, J. W. Brault, R. C. M. Learner, D. A. Newnham, and J. Tennyson, New Studies of the Visible and Near-Infrared Absorption by Water Vapour and Some Problems with the HITRAN Database, *accepted for publication by Geophys. Res. Lett, July 2000*.
4. Talk at HITRAN: D. Belmiloud, R. Schermaul, K. M. Smith, Nikolai F. Zobov, J. W. Brault, R. C. M. Learner, D. A. Newnham, and J. Tennyson, New Studies of the Visible and Near-Infrared Absorption by Water Vapour and Some Problems with the HITRAN Database, *The 6th biennial HITRAN database conference, Harvard-Smithsonian, Centre for Astrophysics, Cambridge, Massachusetts, U.S.A., 19-21 June 2000*.
5. 'Shortwave Absorption by Atmospheric Molecules at High Spectral Resolution', D. Newnham and K. Smith, Invited Talk, Short-Wave Radiative Transfer in the Atmosphere - is it anomalous?, *Royal Meteorological Society Physical Processes Specialist Group Meeting, Rutherford Appleton Laboratory, U.K. (14 February, 2000)*.
6. Talk: 'Investigating the Absorption of Solar Radiation in Earth's Atmosphere', K. M. Smith, *Bruker FT-IR Users' Meeting 2000, Bruker UK, Coventry, U.K. (27 June, 2000).*
7. 'High-Resolution Short-Wave Absorption by Water Vapour and Molecular Oxygen in the Clear-Sky Atmosphere', D. A. Newnham and K. M. Smith, *Poster (Session I: Weather and Climate Applications) and Conference Proceedings, International Radiation Symposium (IRS) 2000, St Petersburg, Russia (24-29 July, 2000)*.